Assessing Impulses and Decay of Overshooting Tops Relative to Supercell Collapse using Lightning and Phased Array Radar Data

Vanna Chmielewski[1], Kristin Kuhlman[2, 3], Don MacGorman[3], and Stephanie Weiss[4]

[1]University of South Alabama
Mobile, Alabama

[2]Cooperative Institute for Mesoscale Meteorological Studies
University of Oklahoma, Norman, Oklahoma

[3]National Oceanic and Atmospheric Association / National Severe Storms Laboratory
Norman, Oklahoma

[4]School of Meteorology
University of Oklahoma, Norman, Oklahoma

ABSTRACT

The overshooting tops of seven tornadic supercell storms occurring in central Oklahoma were examined using data from the Oklahoma Lightning Mapping Array (LMA), the National Weather Radar Testbed Phase-Array Radar (PAR), and surrounding National Weather Service WSR88-D radars. The growth and decay of the overshooting tops in both the lightning and reflectivity data were noted relative to the times of tornadoes reported for each storm. The lightning signatures of the overshooting top were seen only in storms that reached at least 13 km MSL, typically in the warm season when the tropopause tends to be higher. The rate of mapped lightning points in the overshooting top was much smaller than the rates seen for flashes lower in the storm and often consisted of isolated points separated by tens to hundreds of milliseconds. The VHF sources likely associated with lightning in the overshooting top exhibited cycles of growth and decay similar to cycles seen in reflectivity, driven by the evolution of the storm's updraft. In most cases, the signature of an overshooting top appeared in radar data before it appeared in lightning data. The most concentrated areas of activity were immediately downstream of and within the overshooting top in areas having reflectivity of 20-40 dBZ. Of the 14 tornadoes that occurred during the storms studied, 11 immediately followed or coincided with a decrease in the height or occurrences of lightning in the overshooting top, along with less noticeable decreases in the height of the radar echo top. Of the seven storms studied, six showed lightning impulses at the base of the overshooting top 3-25 min before the formation of the first tornado. The exception was a storm that produced only a weak tornado.

1. INTRODUCTION

When Browning (1965) suggested that a rotating updraft seen as a hook echo on radar was necessary for tornadogenesis, the classic thunderstorm model of Byers and Braham (1948) was supplemented to account for such a possible "severe" stage of development, where the storm moves to the right of the mean flow of the winds. Since then, there has been much interest in better noticing the first signs of a storm with the potential to produce tornadoes. One possible indicator of a strong storm that could produce severe weather is the presence of an overshooting top. Current research (e.g., Bedka et al., 2010) is directed towards the automated sensing of overshooting tops.

The first stage of thunderstorm development, its initial formation, is considered to

[1] *Corresponding author address:* Vanna Chmielewski, 101 Foreman Rd, Apt B10, Mobile, AL, 36608, vanna.chmielewski@noaa.gov

be consisting entirely of updrafts (Lemon and Doswell, 1979), which allows for an initial increase in the height of the storm. The second stage of thunderstorm development allows for further intensification and rising storm tops, including the possible presence of an overshooting top. Browning (1965) suggested adding a Severe Right Mature stage during this period if a storm shows signs of a mesocyclone capable of producing severe weather. The storm top eventually lowers as the updraft weakens, indicating the collapse phase of the supercell (Lemon and Dowell, 1979) or the beginning of a new updraft (Lemon, 2009).

Brandes (1978) first concluded that tornadogenesis is concurrent with the breakdown of the mesocyclone, when the storm tops would either be constant or decreasing. Many studies have shown examples of tornadogenesis associated with storm top lowering caused by a disruption or breakdown of the mesocyclone (e.g. Dowell and Bluestein, 1997, Lemon, 2009, Adler and Fenn, 1981). Lemon and Doswell (1978) and Lemon (2009) also discussed examples of tornadoes already on the ground that strengthened when their storm cells began to collapse. Adler and Fenn (1981), however, also found examples of tornadoes that were accompanied by rising storm tops.

A feature recently noticed in the overshooting top of a supercell, is the occurrence of unique lightning (Lyons et al., 2003, MacGorman et al., 2008). This lightning has been observed to occur in spring and summer thunderstorms reaching at least 13 km, but not much study have been directed towards their occurrence.

2. DATA AND METHODOLOGY

The Oklahoma Lightning Mapping Array (OK-LMA) was used to obtain lightning data (MacGorman et al., 2008). The LMA maps the very high frequency (VHF) radiation source points emitted by lightning in three-dimensional space within 100 km of the center of the network (Fig. 1). The accuracy the system is 6-12 m in the horizontal and 20-30 m in the vertical with errors increasing with increasing range from the network center (Thomas et al., 2004).

For the most detailed radar imagery, several radars around Oklahoma were utilized. The National Weather Radar Testbed Phased Array Radar (PAR) was used whenever possible, (see Zrnic et al., 2007, for a detailed description of the system's specifications). One of the largest benefits of using the PAR is that it can complete an entire volume scan in less than a minute for a 90 degree sector. The current scanning strategies also provide more vertical resolution, including higher elevations in closer proximity to the radar than a standard Weather Service Radar (WSR-88D) provides in its longer scan time (Heinselman et al., 2008, Zrnic et al., 2007).

Since the current PAR can only scan a 90 degree sector at a time, it may not be able to examine an entire storm or multiple storms at the same time. To provide data for unsampled areas of the selected storms, the data from the PAR were supplemented by local WSR-88D radars. Furthermore, since all of the storms chosen were within the 100 km radius of the OK-LMA network center, many were too close to the PAR or KTLX (Oklahoma City WRS-88D) for full vertical sampling. Data from other radar sites were used to view any unsampled sections of the storms. The following standard NEXRAD radar sites covering portions of the radius were used in conjunction with PAR and KTLX: KINX, KFDR, KSRX and KVNX (located in Tulsa, Frederick, Western Arkansas and Vance Air Force Base, respectively, e.g. Fig. 2).

The data from the multiple radars were quality controlled and overlaid using a merger made for the WDSS-II (Warning Decision Support System-Integrated Information) (Lakshmanan et al., 2006, 2007). The merger combined the data from the different radar sites into a single high-resolution, three-dimensional grid, in approximately two minute intervals. The merged product mitigates issues caused by the radar geometry, such as the "cone of silence" (Lakshmanan et al., 2006).

To provide a sampling of warm-season tornadic supercell storms that occurred in central Oklahoma 2006-2010, data were obtained from several sources besides the PAR, including the Storm Prediction Center (SPC) and National Climatic Data Center (NCDC). All of the storms in this study produced at least one tornado within the 100 km radius of the OK-LMA network center. Seven storms were chosen (as shown in Table 1), three of which occurred on 10 May 2010. This dataset included two short-lived storms: a weaker supercell ahead of a convective line on 7 May 2007 and a breifly tornadic storm occurring near Yukon on 10 May 2010. Together, the storms produced 14 tornadoes within the study area.

The study times were limited to the lifespan of the mature stage of the supercell for the two short-lived storms mentioned previously and to the time period of the first tornadoes produced within the study area by the longer-lived storms.

PAR and OK-LMA data were provided by the National Severe Storms Laboratory (NSSL). Data from the selected WSR-88D radar sites (KTLX, KINX, KFDR, KSRX and KVNX) were gathered from the NCDC. The reflectivity data from the NEXRAD radars and the PAR were then quality controlled and merged via the WDSS-II algorithm, w2merger (Lakshmanan et al., 2006). The merged reflectivity product was then used to determine the height of the 30 dBZ reflectivity layer within the overshooting top. This height and the highest reflectivity values seen at the base of the overshooting top were used as guidance to determine the increase and decrease in strength of the overall reflectivity signature of the overshooting top (also referred to as impulse and decay patterns).

For each 1-min interval, a mapped VHF sources from the OK-LMA were overlaid on the merged reflectivity product using WDSS-II. The locations of lightning activity near the overshooting top were noted with respect to the radar signature of the overshooting top. The continuously changing distributions of lightning locations and rates were also plotted separately to examine the evolution of lightning without being limited to resolution of the 1-min overlays of radar reflectivity.

3. OBSERVATIONS

3.1 *Lightning*

All of the selected storms showed lightning activity in the overshooting top. This upper lightning activity consisted of a low density of continual VHF source points, each typically isolated tens to hundreds of milliseconds from its most recent neighbor (e.g., Fig. 3), as opposed to the frequent flashes lower in the storm, which were more episodic and typically consisted of tens to hundreds of points (Fig. 4). The source points in the overshooting top generally appeared to be independent of flashes lower in the core of the storm, suspended 2-4 km above the storm core activity. Individual flashes comprised of multiple VHF source points were sometimes seen in the overshooting top as well, most frequently during the 31 March 2008 storm. These larger flashes generally consisted of up to ten VHF source points and began in the core of the overshooting top and then extended towards or away from the rest of the lightning activity in the storm.

Almost all of the storms showed similar “impulse” patterns within the lightning signature of the overshooting tops, with the exception of the 7 May 2007 storm. These impulses generally began with source points originating within 1-3 km of lightning flashes in the core. The source points increased in height with time, generally reaching the highest altitude within 2-5 minutes from the beginning of the impulse (Fig. 5). These impulses lasted anywhere between 3 and 12 minutes, and in many cases began before the previous impulse had dissipated.

Generally, the source points within the overshooting top covered the largest horizonatal area near the mean altitude of elevated activity, spreading quickly downstream at roughly this mean altitude. However, there was no common pattern in the number of occurrences of VHF source points with regard to the stage of the impulse. In many instances, especially during the 31 March 2008 and the 10 May 2010 Moore storms, the impulse of source points began in a narrow, stem-like area that extended from the upper reaches of the core of the storm to the area of activity in the overshooting top. As previously noted, the 7 May 2007 storm did not contain these impulse patterns, but instead showed constant activity of single VHF source points within the region of the overshooting top.

3.2 *Lightning and Radar Relationship*

There were some inherent problems in relating the lightning activity with the radar signatures because of the time differences. The merged radar product gridded reflectivity values on approximately two minute intervals, while the lightning source points overlaid on the merged product updated at one-minute intervals. Therefore, we did not attempt a detailed analysis of the evolution of lightning relative to radar reflectivity on shorter time scales in the overshooting top.

The VHF source points were found in similar areas of the overshooting top in all of the supercell cases. Most of the points corresponded with areas of 20-40 dBZ reflectivity values. The outliers were either at lower altitudes than the rest of the elevated activity or a large distance from the overshooting top. The highest concentration of source points was generally found near the base of the overshooting top on its downstream side (Fig. 6 and Fig. 7), with source points distributed both downstream and over the overshooting top, still within the 20-40 dBZ echo.

In all cases, except the 10 May 2010 Norman storm which experienced extremely rapid development, the radar signature of the overshooting top was visible before the lightning signature. After the development of the lightning signature, a lightning impulse could precede an increase in the radar reflectivity signature of the overshooting top. The 10 May 2010 Moore cell exhibited this behavior multiple times (see Fig. 8, Fig. 9, and Fig. 10). More frequently, however, a lightning impulse would follow or coincide with a strengthening of the radar signature. Note that the elapsed time between the onset of a lightning pulse and of a radar pulse in an overshooting top sometimes was within 3 min and could not be clearly observed with the limited update times available, so no full conclusions can be drawn about the relative timing of lightning and reflectivity pulses.

3.3 *Overshooting Top Signatures and Tornadogenesis Relationship*

Of the seven studied storms, six showed at least one significant lightning impulse in the overshooting top before the storm produced its first tornado. The one case that did not, 7 May 2007, produced two EF0 tornadoes. This storm did show lightning activity in the overshooting top, but was more continuous in nature with no defined impulse patterns. The Norman storm on 10 May 2010 was unique in having only one impulse in the lightning signature that preceded the first tornado; in this case, the impulse preceded the touchdown of the tornado by only three minutes. The other five storms showed multiple lightning impulse patterns occurring as much as 25 minutes before the touchdown of the first tornado.

Of the 14 total tornadoes, 11 occurred during a (sometimes small) collapse of the radar signature and a more noticeable decrease in either the height or density of the lightning activity in the overshooting top. The changes in the radar signatures differed greatly between these tornadoes, with height drops of the 30 dBZ level of 1-3 km. It should be noted that some of the smaller height changes may be within the margin of error caused by the radar merger. During the time period when the longer lived tornadoes were on the ground, the height of the radar signature changed more frequently than the height of the lightning pattern, which remained relatively suppressed during the tornadoes.

The 11 aforementioned tornadoes occurred either as the lightning activity within the overshooting top began to decrease in height or density or within minutes of the dissipation of an impulse. For longer lived tornadoes, significantly smaller amounts of lightning activity occurred while the tornadoes remained on the ground, but activity typically increased again within roughly two minutes of the tornado end time. For example, the 25 April 2006 storm in El Reno had several distinct impulses dissipate before the first tornado formed. Only one small impulse was seen while the tornado was on the ground and ended when a second tornado formed. No other impulses were seen until after both tornadoes dissipated. The only storm that showed any significant lightning activity during a long lived tornado was the 10 May 2010 Norman storm, which showed one significant lightning impulse during a time period when 3 tornadoes were on the ground.

4. CONCLUSION

During this preliminary study of the lightning in overshooting tops, several points were noticed. All of the storm tops reached 13 km MSL and occurred during spring and early summer. It is likely that at these peak elevations, a smaller region of charge buildup was needed to produce a discharge than at the lower altitudes of the storm core (McCarthy and Parks, 1992). This lightning had been observed to consist mostly of individual VHF source points that were not connected to lightning in the core of the storm. These points also occurred at a lower frequency than was seen in lightning in the rest of the storm, but showed general impulse patterns may have been tied to the strength of the storm's updraft.

The VHF source points within the overshooting top seemed to be generally concentrated in similar areas with respect to radar reflectivity patterns, and did not typically appear until after the overshooting top signature was present in radar reflectivity. The singular VHF source points were mostly within the 20-40 dBZ contours of radar reflectivity. The highest concentration of the VHF source points was within and just downstream of the overshooting top.

Of the seven storms studied, six showed lightning impulses at the base of the overshooting top 3-25 minutes before the first case of tornadogenesis, the exception being a storm that produced two EF0 tornadoes. The decrease in the height of radar reflectivity in the overshooting top coincided with tornadogenesis in 11 of the 14 observed cases. In the same 11 cases, the decrease in either the number or height of impulses in the overshooting top also coincided with tornadogenesis, but the change was typically more pronounced than the change in radar reflectivity. Out of these 11 cases, there was significantly less lightning activity within the overshooting top during the long-lived tornadoes than was present in the storm before tornadogenesis or after dissipation.

As Darden et al. (2010) explains some forecasters are already working on incorporating real-time lightning data into their warning decisions; however, more research must be done before the operational uses of the lightning activity within overshooting tops can be realized. This study also focused solely on tornadic supercells, and lightning within the overshooting top has also been seen in storms that do not produce tornadoes, severe wind or hail. The properties of lightning in overshooting tops must also be examined in these non-tornadic storms for any true operational impacts to be realized.

5. ACKNOWLEDGMENTS

The authors thank Keli Tarp and Kevin Manross their assistance and guidance. The research was performed under appointment to the National Oceanic and Atmospheric Administration Ernest F. Hollings Undergraduate Scholarship Program administered by Oak Ridge Associated Universities through a Cooperative Grant sponsored by the National Oceanic and Atmospheric Administration.

6. REFERENCES

Adler, R. F., and D. D. Fenn, 1981: Satellite-Observed Cloud-Top Height Changes in Tornadic Thunderstorms. J. Appl. Meteor., **20**, 1369-1375.

Bedka, K., J. Brunner, R. Dworak, W. Feltz, J. Otkin, and T. Greenwald, 2010: Objective Satellite-Based Detection of Overshooting Tops Using Infrared Window Channel Brightness Temperature Gradients. *J. Appl. Meteor. Climatol.*, **49**, 181-202.

Brandes, E. A., 1978: Mesocyclone Evolution and Tornadogenesis: Some Observations. *Mon. Wea. Rev.*, **106**, 995-1011.

Browning, K. A., 1965: The Evolution of Tornadic Storms. *J. Atmos. Sci.*, **22**, 664-668.

Byers, H. R., and R. R. Braham Jr., 1948: THUNDERSTORM STRUCTURE AND CIRCULATION. *J. Meteor.*, **5**, 71-86.

Darden, C. B., D. J., Nadler, B. C. Carcione, R. J. Blakeslee, G. T. Stano, and D. E. Buechler, 2010: Utilizing Total Lightning Information to Diagnose Convective Trends. *Bull. Amer. Meteor. Soc.*, **91**, 167-175.

Defer, E., P. Blanchet, C. Théry, P. Laroche, J. E. Dye, M. Venticinque, and K. L. Cummins, 2001: Lightning activity for the July 10, 1996, storm during the Stratosphere-Troposphere Experiment: Radiation, Aerosol, and Ozone-A (STERAO-A) experiment. *J. Geophys. Res.*, **106**, 10151–10172, doi:10.1029/2000JD900849.

Dowell, D. C., and H. B. Bluestein, 1997: The Arcadia, Oklahoma, Storm of 17 May 1981: Analysis of a Supercell during Tornadogenesis. *Mon. Wea. Rev*., **125**, 2562-2582.

Heinselman, P. L., D. L. Priegnitz, K. L. Manross, T. M. Smith, R. W. Adams, 2008: Rapid Sampling of Severe Storms by the National Weather Radar Testbed Phased Array Radar. *Wea. Forecasting*, **23**, 808-824.

Krehbiel, P. R., R. J. Thomas, W. Rison, T. Hamlin, J. Harlin, and M. Davis, 2000: GPS-Based Mapping System Reveals Lightning Inside Storms. *Eos, Trans. Amer Geophys. Union*, **81**, 21-25.

Lakshmanan, V, T. Smith, K. Hondl, G. J. Stumf, and A. Witt, 2006: A Real-Time, Three-Dimensional, Rapidly Updating, Heterogeneous Radar Merger Techniqu for Reflectivity, Velocity, and Derived Products. *Wea. and Forecasting*, **21**, 802-823.

Lakshmanan, V., T. Smith, G. Stumpf, and K. Hondl. 2007: The Warning Decision Support System-Integrated Information. *Wea. And Forecasting*, **22**, 596-612.

Lemon, L. R., and C. A. Doswell III, 1979: Severe Thunderstorm Evolution and Mesocyclone Structure as Related to Tornadogenesis. *Mon. Wea. Rev.*, **107**, 1184-1197.

Lemon, L. R., 2009: Supercell collapse. 34th Conf. on Radar Meteor., Amer. Meteor. Soc., Williamsburg, VA.

Lemon, L. R., D. W. Burgess, and R. A. Brown, 1978: Tornadic Storm Airflow and Morphology Derived from Single-Doppler Radar Measurements. Mon. Wea. Rev., **106**, 48-61.

Lyons, W. A., T. E. Nelson, R. A. Armstrong, V. P. Pasko, and M. A. Stanley, 2003: Upward Electrical Discharges From Thunderstorm Tops. Bull. *Amer. Meteor. Soc.*, **84**, 445-454.

MacGorman, D. R., W. D. Rust, C. L. Ziegler, E. R. Mansell, T. J. Schuur, M. I. Biggerstaff, J. M. Straka, E. C. Bruning, K. M. Kuhlman, N. R. Lund, C. Payne, N. S. Biermann, W. H. Beasley, L. D. Carey, P. R. Krehbiel, W. Rison, and K. B. Eack, 2008: TELEX The Thunderstorm Electrification and Lightning Experiment. *Bull. Amer. Meteor. Soc.*, **89**, 997-1013.

McCarthy, M. P., and G. K. Parks, 1985: Further Observations of X-Rays Inside Thunderstroms. *Geophys. Res. Lett.*, **12**, 393-396.

SRI International. *NEXRAD Radar Locations.* NOAA's National Weather Service Radar Operations Center. Web. 30 July 2010.

Thomas, R. J., P. R. Krehbiel, W. Rison, S. J. Hunyady, W. P. Winn, T. Hamlin, and J. Harlin, 2004: Accuracy of the Lightning Mapping Array. *J. Geophys. Res.*, **109**, D14207, doi:10.1029/2004JD004549.

Wiens, K. C., S. A. Rutledge, S. A. Tessendorf, 2005: The 29 June 2000 Supercell Observed during STEPS. Part II: Lightning and Charge Structure. *J. Atmos. Sci.,***62**, 4151-4177.

Zrnic, D. S., J. F. Kimpel, D. E. Forsyth, A. Shapiro, G. Crain, R. Ferek, J. Heimmer, W. Benner, T. J. McNellis, R. J. Vogt, 2007: Agile-Beam Phased Array Radar for Weather Observations. *Bull. Amer. Meteor. Soc.*, **88**, 1753-1766.

7. TABLES

Table 1. Dataset used for this study and corresponding tornado strengths and locations (NR=Not Rated at the time of this study)

Date	Time (UTC)	Strength	Location	
04/25/2006	0000-0050	F1, F1	El Reno	
05/07/2007	0200-0240	EF0, EF0	Seminole Co.	Weak supercell
03/31/2008	0600-0655	EF0, EF1	Edmond	
05/24/2008	1900-2005	EF1, EF2	Lacey	
05/10/2010	2130-2155	NR	Yukon	Short-lived storm
05/10/2010	2155-2240	EF4, NR	Moore	
05/10/2010	2225-2305	EF4, EF1, EF2	Norman	

8. FIGURES

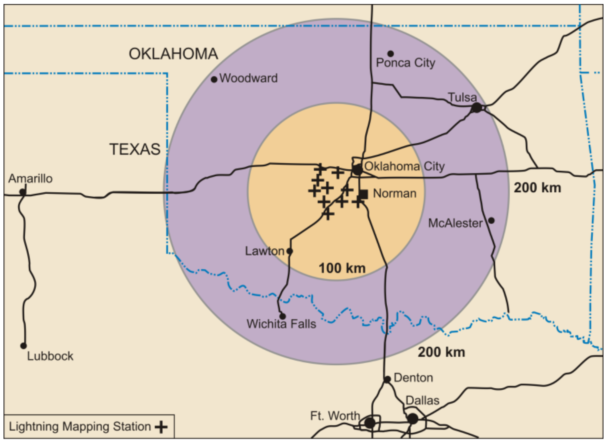

Fig. 1. The three-dimensional mapping range of OK-LMA is represented by the inner, orange circle. The two dimensional range is represented by the outer, purple circle. The locations of OK-LMA stations are also shown.

Fig. 2. The locations of WSR-88D sites that were used are shown with their corresponding ranges (SRI International)

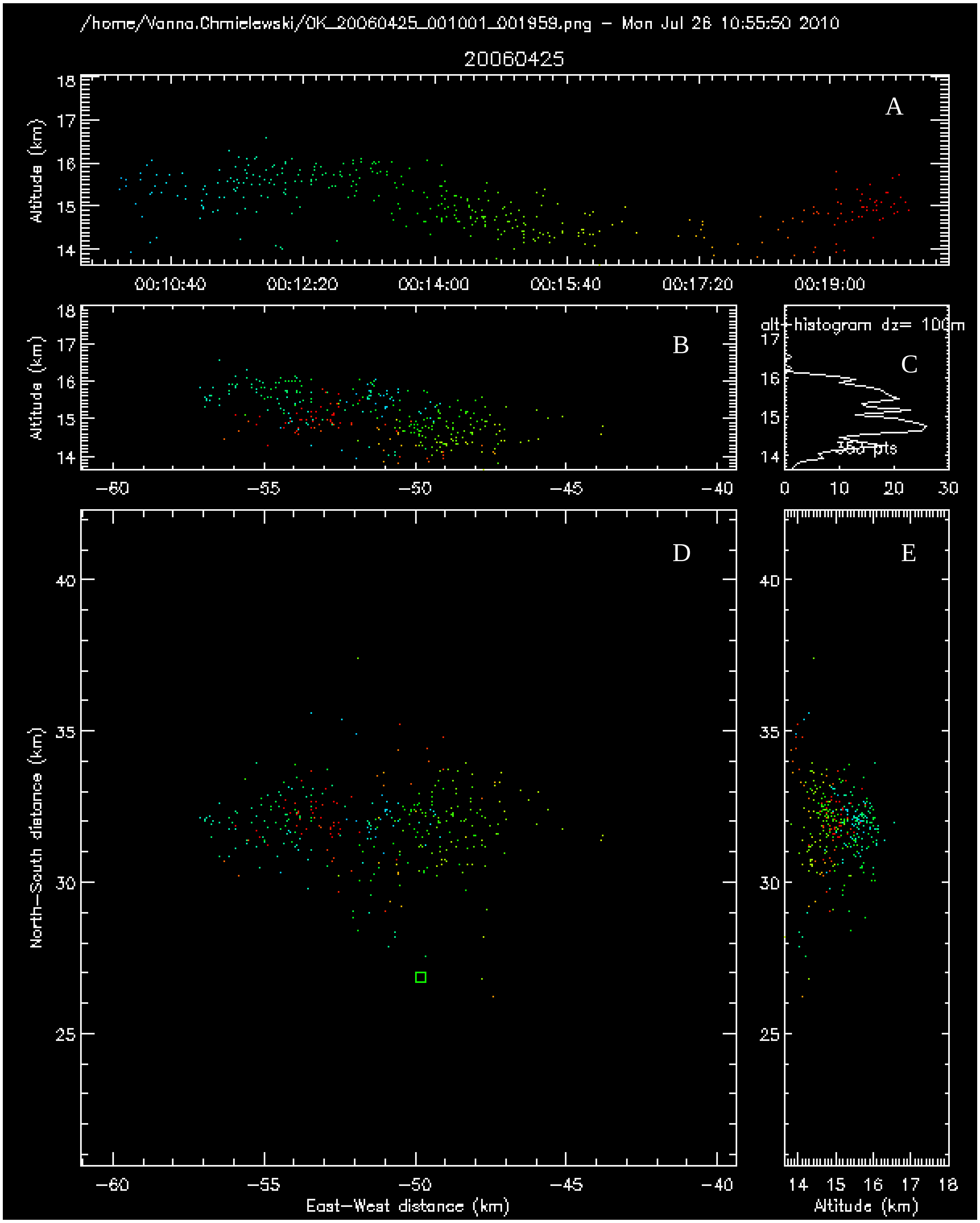

Fig. 3. Map of only the LMA sources within the upper part of the storm on April 25, 2006 from 0010-0020 UTC showing sources by A) time and height, B) height and east-west plane, C) histogram of by height, D) horizontal plane, and E) north-south plane and height. The green square (D) represents the location of an OK-LMA sensor station. The colors seen represent the time of the source as shown in (A).

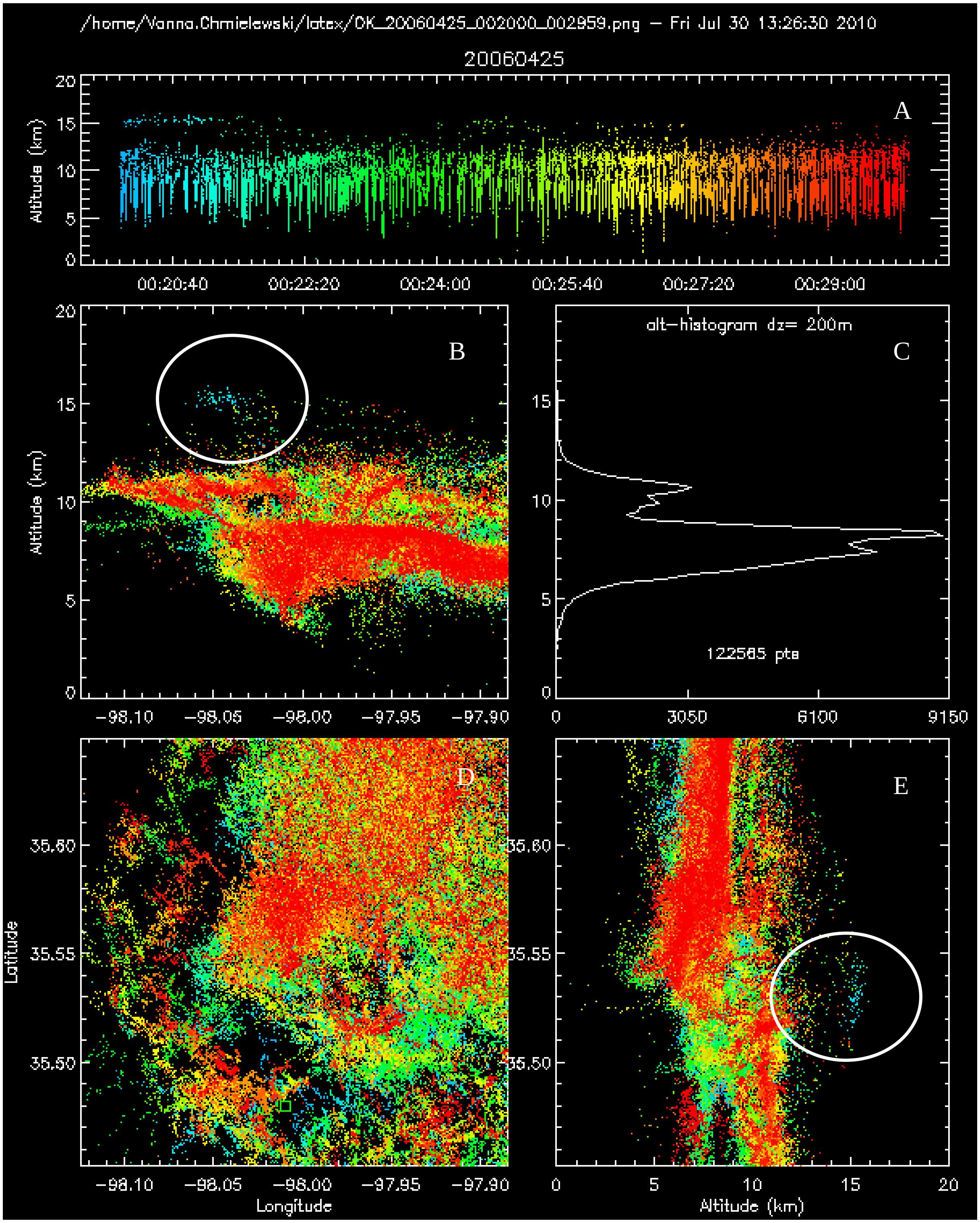

Fig. 4. Same as Fig. 3 but for 0020-0030 UTC, showing the vertical column underneath the overshooting top (shown in the circled area)

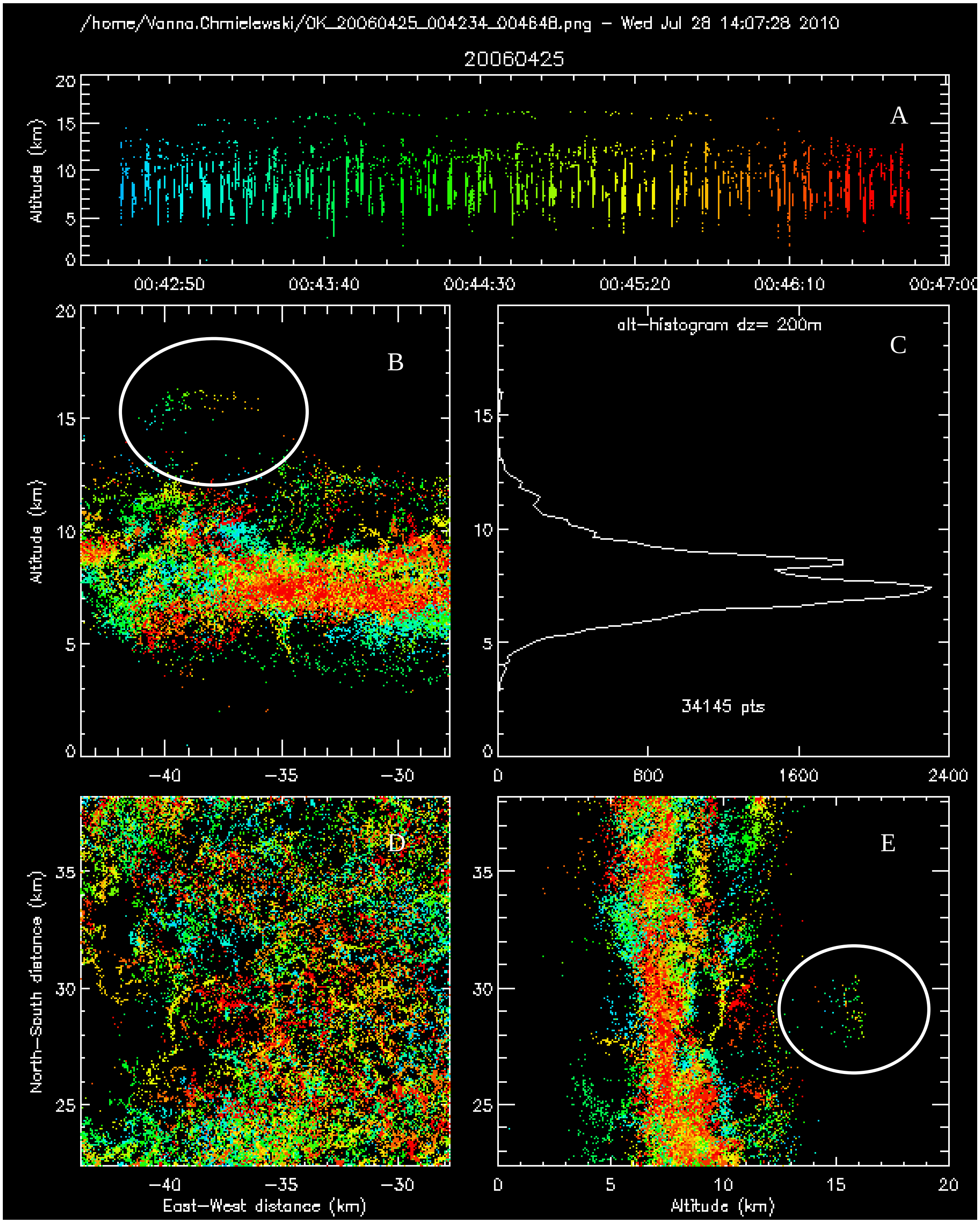

Fig. 5. Same as Fig. 3 but for 00:42:30-00:47:00 UTC. Note how the elevated sources originate at a lower altitude and increase in height, with the area remaining active for about three minutes.

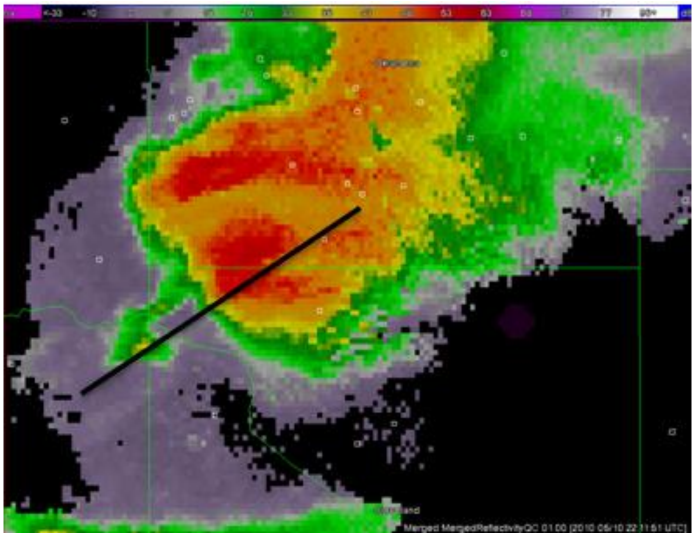

Fig. 6. Lowest level merged reflectivity product from May 10, 2010 at 2211 UTC showing the Moore storm. The line represents the cross section seen in Fig. 6.

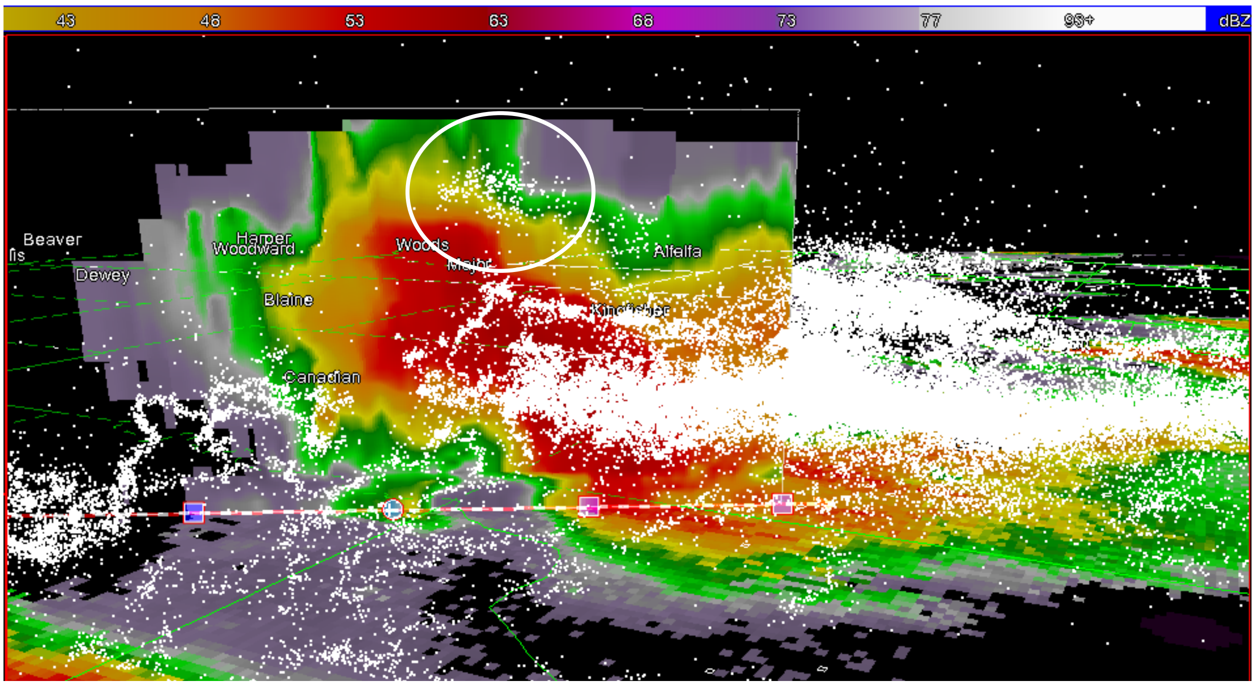

Fig. 7. Merged reflectivity cross-section along line seen in Fig. 5 from southwest to northeast over a tilted view of Fig 5 with the LMA sources superimposed in three-dimensions over the radar image, no sources behind (to the northwest of) the cross section can be seen. Note the sources within the circle on the downstream side of the overshooting top and extending further downstream. Relationships with reflectivity values should not be judged from this image as sources are in three-dimensions and do not lie along the cross section.

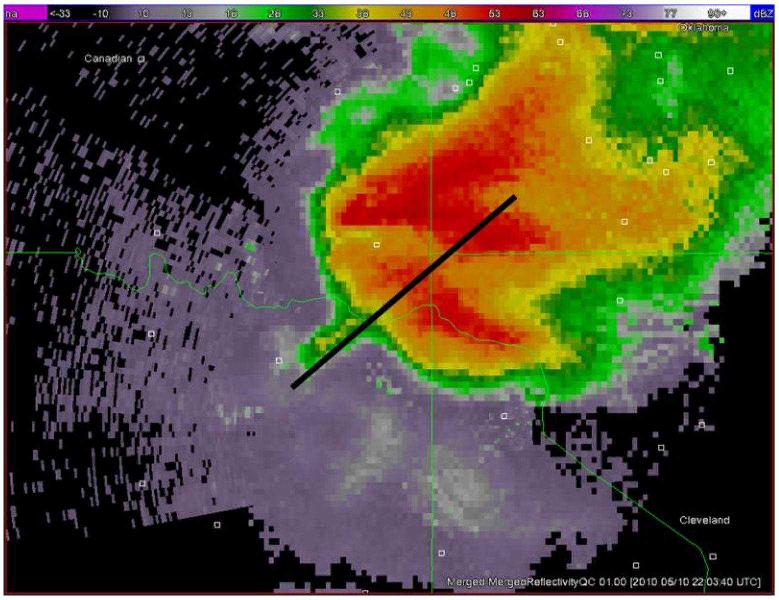

Fig. 8. Lowest level merged reflectivity product from May 10, 2010 at 2203 UTC showing the Moore storm. The line represents the cross section seen in Fig. 9 and Fig. 10.

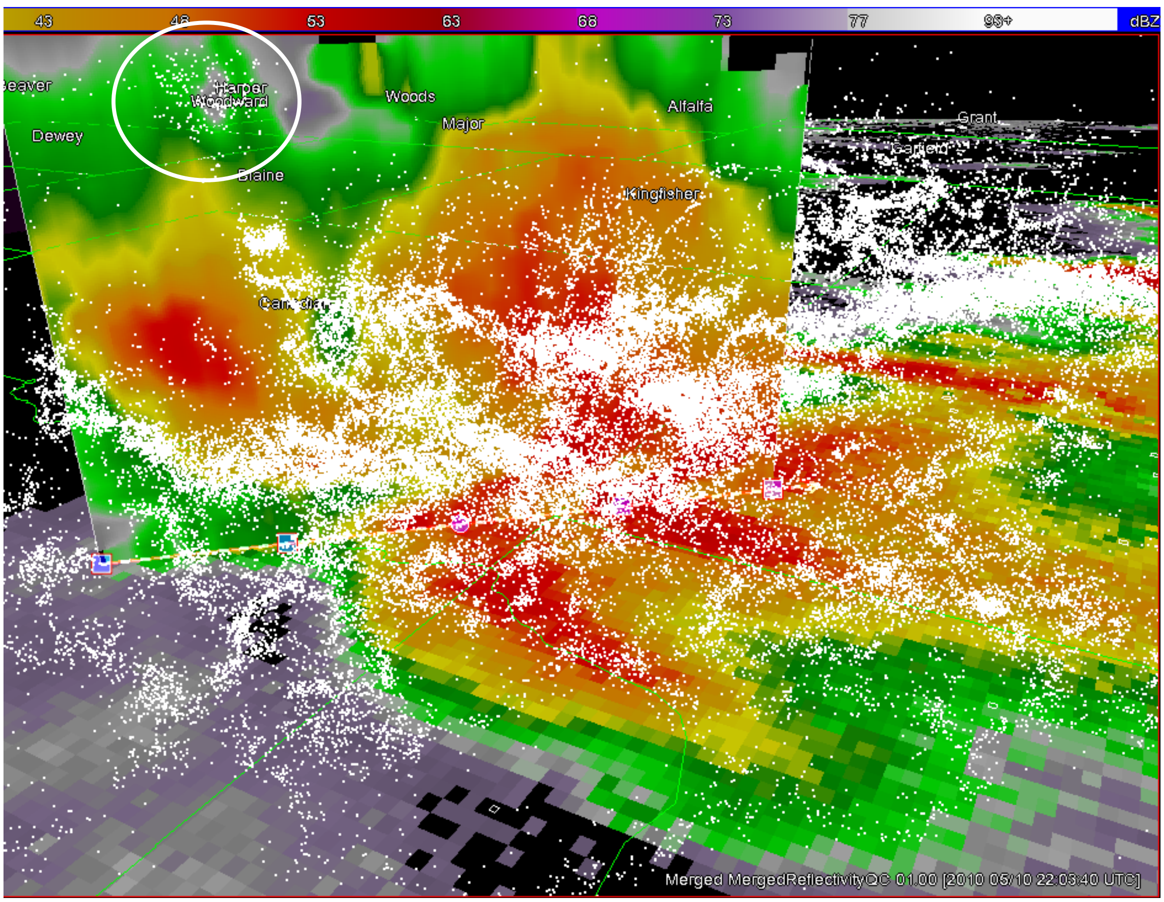

Fig. 9. Same as Fig. 7 but for 2203 UTC along the line drawn in Fig. 8.

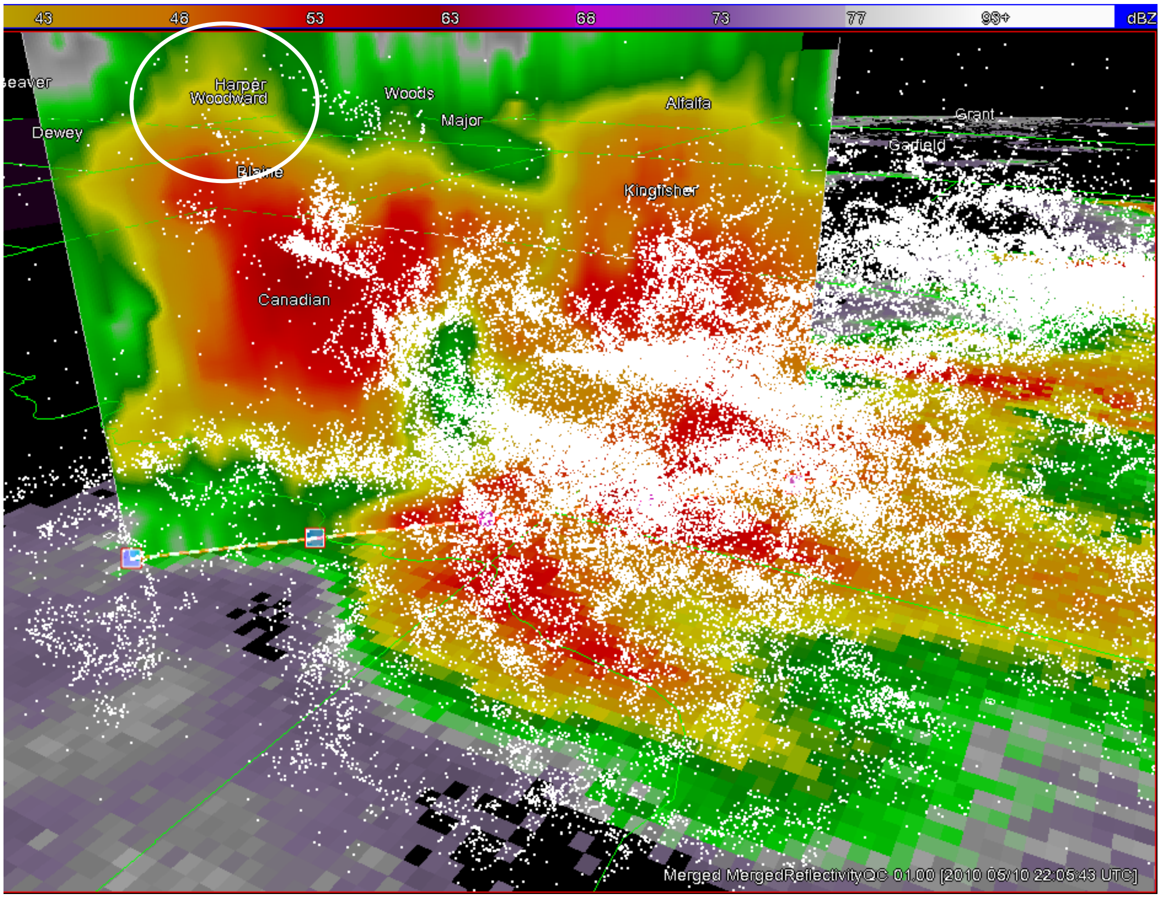

Fig. 10. Same as Fig. 9 but for 2205 UTC. Note how the concentrated LMA sources within the circle seen in Fig. 9 preceded the increase in high reflectivity values seen in the same area in this figure.